Tellus (1979), *31*, 199–216

Numerical experiments with planetary scale mountain barrier waves in a simple model

By P. LANGLEY and D. R. DAVIES, *Mathematics Department, The University of Exeter, North Park Road, Exeter EX4 4QE, England*

(Manuscript received August 17; in final form December 11, 1978)

ABSTRACT

A two-level, σ-coordinate, β-plane, general circulation model (10,000 km meridional and 30,000 km zonal dimensions) is used to study the effect of planetary scale mountain barriers on vacillation of energy and heat transfer. The results of numerical experiments using models with flat topography (and land–sea heating contrasts) are compared with those using model representations of the Rockies and Himalayas. The mountain barriers were seen to have a crucial effect on the time variation of total eddy kinetic energy, K', meridional temperature gradients, ∇T, and in creating the stationary components of poleward transport of heat and westerly momentum. Preferred regions of high meridional temperature gradients and cyclonic systems formed north-east of the Rockies but north-west of the Himalayas. When K' was partitioned into the values appropriate to the western and eastern halves of the β-plane channel, the time variations of K' associated with each half were frequently out of phase; increasing $K'(t)$ in one half and decreasing $K'(t)$ in the other half was related to eastward moving peaks of baroclinic activity (created downstream of a barrier). A similar process was found in an analysis of atmospheric data for 1961–63, the orientation of the polar vortex being closely related to the west-east oscillation of K'; the model results suggest that the mountain barrier system has a large influence. Time variations in regional weather characteristics are likely to be closely related to this process; it is clearly an important factor to be represented in climatic change modelling.

1. Introduction

A primary large-scale atmospheric flow characteristic is its continuously changing nature, expressed concisely by oscillations in the ratio of eddy kinetic energy to zonal kinetic energy, $K'/\bar{K}$; this is known as "vacillation" and was discussed firstly by Fultz (1959) using laboratory experiments and recently by, for example, Quinet (1974) using a numerical model, with no mountain barriers. Due to the non-linear nature of the system there is no exact period of oscillation but numerical experiments exhibit a natural (statistical) periodicity in no-mountain models; a crucial meteorological problem then is to determine the nature of the disturbance created in these oscillations by the insertion of a mountain barrier system.

This basic knowledge could be particularly important in the practical problem of long-range weather forecasting. As stated clearly by McGuirk and Reiter (1976) a search for an underlying characteristic statistical periodicity in atmospheric events is a prime consideration, particularly as there may be basic difficulties in extending the time range of numerical models used for short-period forecasting (due, for example, to the time growth of numerical errors) and in statistical extrapolation (without a clearer dynamical basis). What is urgently needed is a statistical method based on a better understanding of the large-scale dynamical elements.

McGuirk and Reiter (1976) noted recently from available data a frequently occurring periodicity of the order of 24 days in hemispheric scale energy functions during the winter season. This, and similar empirical results, requires a dynamical explanation. One of the important uses of model numerical experiments is to study flow properties in a relatively simple system, involving only the main generating

 0040-2826/79/030199-18$02.50/0

factors likely to influence the particular scale characteristic to be studied. The large-scale vacillation of the atmosphere's energy is likely to be a response depending primarily on an imposed meridional heating gradient (with its consequent climatological balance requirement) together with the interference created by the presence of a mountain barrier system, and by longitudinal variation in heating and surface friction effects caused by continental and oceanic regions.

Smith and Davies (1977), for example, have shown that a (computationally) simple, two-level, quasi-geostrophic, β-plane, general circulation model can be used to study interactions between baroclinic instability waves and the stationary waves created by a single, planetary scale, mountain barrier. Egger (1976 e.g.) has also studied these interactions in a hemispheric model. The large-scale, primary flow characteristics produced in their computer solutions were essentially similar to those discussed in the studies made by Manabe and Terpstra (1974) using their complex model and associated extensive computational demands. The model described by Smith and Davies (1977), has now been modified and the spatial domain extended to a channel approximately 30,000 km (east–west) by 10,000 km (north–south). This simple model (with its relatively economical computer usage) can then be applied to study in detail firstly the effect of single barriers of Rockies and Himalayan type, by analysis of the momentum and heat transfer into transient and stationary components, and the joint effects produced when both barriers are inserted in an approximate scale representation of their actual position. In particular, it is interesting to study the production of lee cyclogenesis downstream of one barrier by successive bursts of dynamical activity and the manner of its interference by the presence of a second barrier: in this way the large-scale interactions between east and west sub-domains of the model can be studied.

The model numerical experiment results are then used as a guide to an analysis of actual data (500 mb and 1000 mb geopotential heights from 1961 to 1963) with a specific objective of searching for a particular form of east–west oscillation in eddy kinetic energy suggested by our model.

2. The model, the computing scheme, and methods of analysis

Following Smith and Davies (1977) the model used is basically a two-level, Phillips (1956) type system, with pressure p replaced by $p/\pi = \sigma$, where π is the surface pressure. Using standard modelling notation, the prediction equations for the relative potential vorticity values, q_1 and q_3, at levels $1(\sigma = 0.25)$ and $3(\sigma = 0.75)$, are

$$\frac{\partial q_1}{\partial t} = -(\mathbf{v}_1 \cdot \nabla) q_1 - \frac{R\lambda^2}{f_0 c_p} \dot{Q}_2 - \beta v_1 + D_1 + F_1 + \eta(\mathbf{v}_s \cdot \nabla)\pi \quad (1)$$

$$\frac{\partial q_3}{\partial t} = -(\mathbf{v}_3 \cdot \nabla) q_3 + \frac{R\lambda^2}{f_0 c_p} \dot{Q}_2 - \beta v_3 + D_3 + F_3 + \eta(\mathbf{v}_s \cdot \nabla)\pi \quad (2)$$

where

$$q_1 = \zeta_1 - \lambda^2(\psi_1 - \psi_3) + \mu_1 \pi \quad (3)$$

and

$$q_3 = \zeta_3 + \lambda^2(\psi_1 - \psi_3) + \mu_3 \pi \quad (4)$$

$\dot{Q}_2$ denotes the radiative and condensational part of the heating function, applied at level 2 $(\sigma = 0.50)$: the constants λ^2, f_0, R, c_p, β, μ_1, μ_3 and the diffusive (D_1 and D_3) and frictional (F_1 and F_3) terms are as defined by Smith and Davies (1977): u and v are the zonal and meridional components of velocity and the functions ψ_1 and ψ_3 are expressed in terms of the geopotential ϕ by $\psi_1 = \phi_1/f_0$, $\psi_3 = \phi_3/f_0$; $\eta = \frac{1}{2}[(\mu_1 - \mu_3)/2 - (c_3 - c_1)\lambda^2]$, where $c_1 = RT_1/\pi$, $c_3 = RT_3/\pi$, and $\mathbf{v}_s = \mathbf{v}_1 - \mathbf{v}_3$, $\mathbf{v}_1$ and $\mathbf{v}_3$ being the vector velocities at levels 1 and 3. The term $\eta(\mathbf{v}_s \cdot \nabla)\pi$ (stemming from an application of of the thermodynamic equation at level 2) which was neglected by Smith and Davies, has been retained; it leads to a 20% increase in computation and although the general characteristics of the computed flow are not materially altered by its inclusion, a greater variability in the ensuing calculated energy changes suggested its retention and the quasi-geostrophic condition was not broken. Tests have shown that the neglected terms listed by Smith and Davies (1977) are generally smaller than those retained, provided the heights of the simulated mountain barrier are less than

3000 m and the surface slopes are kept below 0.002. In particular, the factor RT/π is assumed constant, consistent with the geostrophic velocity, $\mathbf{v}$, assumption that

$$\mathbf{v} = \left(\frac{1}{f_0}\right) \mathbf{k} \wedge \nabla (\phi + c\pi) \tag{5}$$

where $c = RT/\pi$ and $\mathbf{k}$ is a unit vertical vector.

The horizontal structure of the model atmosphere is based on a finite difference grid of i points (west–east) and j points (south–north). Initial values were $i = 78$ and $j = 26$ with grid distances of 400 km both zonally and meridionally. These were subsequently altered so that $i = 88$ and $j = 26$ with grid distances 325 km and 350 km. Cyclic conditions are applied to the flow variables at the western and eastern edges whilst rigid wall conditions (zero normal geostrophic flow) are applied at the northern and southern boundaries. The upper and lower boundary conditions taken are $\dot{\sigma} = 0$, on $\sigma = 1$ and on $\sigma = 0$. A simple form of heating function, $\dot{Q}_2$, was used, varying linearly between the model equator and pole; as in some previous work, the condition that the domain integral of $\dot{Q}_2$ should be kept zero led to an important method of continuously correcting the accumulation of grid point numerical errors. The slope of the $\dot{Q}_2$ line and the values of the "friction" parameters were chosen to enable the model to generate "realistic" surface flow patterns and eddy kinetic energy functions.

The cross sections of the barriers are assumed to have smooth sinusoidal slopes, the height $f(x)$ in the east–west direction being proportional to

$$\frac{1}{2}\left\{1 - \cos\frac{(x - x_1)\pi}{(x_2 - x_1)}\right\} \quad \text{for } x_1 \leqslant x \leqslant x_2,$$

$$f(x) = 1 \quad \text{for } x_2 \leqslant x \leqslant x_4$$

and

$$\frac{1}{2}\left\{1 - \cos\frac{(x_5 - x)\pi}{(x_5 - x_4)}\right\} \quad \text{for } x_4 \leqslant x \leqslant x_5;$$

$$f(x) = 0 \text{ elsewhere}$$

a similar function $g(y)$ defining the profile in the north–south direction; the resultant mountain height is then given by $H(x,y) = h_{\max} f(x) g(y)$, when $h_{\max}$ is the maximum height of the barrier. The values of x_1, x_2, x_4 and x_5 are given later. The computing scheme used was that described by Smith and Davies (1977); this contained a first-order Adams-Bashforth time differencing scheme.

Since the main motivation of the modelling was to study the stationary features produced in the model atmosphere by orographic and thermal forcing, programmes were prepared which partitioned the poleward transfer of sensible heat and of westerly momentum, and the kinetic energy, into stationary and transient components; the time period of averaging was generally taken to be 30 model days, enabling comparisons to be made with atmospheric data given by Oort and Rasmusson (1971) for average monthly values during the period from May 1958 to April 1963.

Temporal and spatial averages were defined as follows. A time average of some quantity $A(t)$, at a fixed spatial location and evaluated over $t = t_0$ to $t = t_1$, is given by

$$[A] = \frac{1}{(t_1 - t_0)} \int_{t_0}^{t_1} A(t)\, dt \tag{6}$$

and the *transient* component at time $t_2 (t_0 \leqslant t_2 \leqslant t_1)$ is given by

$$A^*(t_2) = A(t_2) - [A] \tag{7}$$

The *zonal* component of A, at a given time and at a given grid-latitude y and averaged over the range $x_0 \leqslant x \leqslant x_1$, is given by

$$\bar{A}(y) = \frac{1}{(x_1 - x_0)} \int_{x_0}^{x_1} A(x,y)\, dx \tag{8}$$

and the eddy component at the point (x,y) associated with $\bar{A}(y)$ is defined (in keeping with Phillips' notation, 1956) by

$$A'(x,y) = A(x,y) - \bar{A}(y) \tag{9}$$

Averaging the northward flux of sensible heat over a given period of time and around a line of latitude at level 2 then leads to a partitioning into zonal and eddy components

$$\overline{[v_2 T_2]} = \overline{[v_2'][T_2']} + \overline{[v_2^{*\prime} T_2^{*\prime}]} + [\bar{v}_2][\bar{T}_2] + [\bar{v}_2^* \bar{T}_2^*] \tag{10}$$

If the zonal averaging is taken across the whole channel width then the last two terms vanish due to cyclic continuity and the sensible heat flux reduces to

$$\overline{[v_2 T_2]} = \overline{[v_2'][T_2']} + [v_2^{*\prime} T_2^{*\prime}] \tag{11}$$

the first term on the right-hand side representing the stationary flux and the second term the transient flux of sensible heat due to the large-scale eddies of the model atmosphere. The corresponding equation for the northward flux of westerly momentum is

$$\overline{[v_l u_l]} = \overline{[v_l']}\,\overline{[u_l']} + \overline{[v_l^{*\prime} u_l^{*\prime}]} \tag{12}$$

when $l = 1$ or 3.

The available potential and kinetic energies can be similarly partitioned in the model. Following Lorenz (1955), an expression for the available potential energy in a two-level σ coordinate system is found to be

$$P = \frac{\pi}{4g} \lambda^2 \overline{(\Psi_1' - \Psi_3')^2} \tag{13}$$

where the bar signifies a domain averaged value over a σ surface and the prime a deviation from this. Ψ_1' and Ψ_3' refer to the geostrophic stream function associated with eq. (5), given by $\Psi_l = (\phi_l/f_0 + c_l\pi)$. Thus, it is seen that the source of available potential energy is necessarily restricted to that part of the model atmosphere lying between $\sigma = 0.25$ and $\sigma = 0.75$.

The kinetic energy K can be defined in the conventional form and calculated at the dynamical levels 1 and 3. Both K and P are conveniently partitioned into zonal and eddy components: $\bar{K}$, K' and $\bar{P}$, P'. Expressions for energy transformations can be obtained following the procedure and notation of Phillips (1956), and correspond, on the whole, to those derived for pressure coordinate systems. However, there are some differences which arise in the evaluation of the direct interchange between zonal and eddy forms of kinetic and available potential energy. The internal energy changes corresponding to those in Phillips' system are:

$$\{\bar{P}\cdot\bar{K}\} = -mf_0 \int \bar{\dot{\sigma}}_2\, \bar{\Psi}_D\, dS \tag{14}$$

$$\{P'\cdot K'\} = -mf_0 \int \dot{\sigma}_2'\, \bar{\Psi}_D'\, dS \tag{15}$$

$$\{\bar{P}\cdot P'\} = -\tfrac{1}{2}m\lambda^2 \int \overline{v_2'\Psi_D'}\,\overline{\frac{\partial \Psi_d}{\partial y}}\, dS \tag{16}$$

and

$$\{\bar{K}\cdot K'\} = \tfrac{1}{2}m \int \left[\bar{u}\frac{\partial}{\partial y}(\overline{u_1'v_1'}) + \bar{u}_3\frac{\partial}{\partial y}(\overline{u_3'v_3'})\right] dS \tag{17}$$

where $\Psi_D = \Psi_1 - \Psi_3$ and the integration, dS, is over a σ-surface; $m = 8.64 \times 10^5$ so that the units are KJ m^{-2} day^{-1}.

However, there are also energy changes arising from the surface pressure term in the equations of motion, which lead to the additional transformations,

$$\{\bar{P}\cdot P'\}_\pi = -m\eta \int (\bar{u}_1 - \bar{u}_3)\, \overline{v_2'\pi'}\, dS \tag{18}$$

and

$$\{\bar{K}\cdot K'\}_\pi = \frac{mf_0}{2\pi} \int (\bar{u}_1 \overline{v_1'\pi'} + \bar{u}_3 \overline{v_3'\pi'})\, dS \tag{19}$$

Expressions (18) and (19) are to be added to (16) and (17) respectively to obtain the total model conversion formulae.

The additional transformations (18) and (19) arising in σ coordinate models are dynamically interesting in that they include the direct effect of the solid surface boundary in diverting the air flows over and around the mountain barrier systems. Pressure coordinate systems do not reflect this important factor of atmospheric flow as the surface boundary is necessarily a pressure surface, e.g. 1000 mb. Consequently (18) and (19) are important in indicating the difference between σ and p coordinate systems when surface orography is to be included in general circulation systems.

The signs of the extra contributions in (18) and (19) are seen to be determined essentially by the sign of the terms $\overline{v_l'\pi'}$, $l = 1$ and 3; a positive sign would lead to $\{\bar{K}\cdot K'\}_\pi > 0$ and $\{\bar{P}\cdot P'\}_\pi < 0$; the reverse will be true if $\overline{v_l'\pi'}$ is negative. If there are no mountains present, then the sign of $\overline{v_l'\pi'}$ is found to be strongly dependent on the tilt of the pressure system as height increases. This tilt is dominantly to the west (associated with a pressure wave leading a temperature wave) with $\overline{v_l'\pi'}$ negative, which is consistent with a $K' \to \bar{K}$ and $\bar{P} \to P'$ type of energy conversion. Hence in experiments with no orography the secondary energy conversion (i.e. those associated with changes in π) generally act in the same direction as the primary conversions, i.e. $K' \to \bar{K}$ and $\bar{P} \to P'$.

However, this result is significantly altered by the presence of mountain barriers. The surface pressure, π, in mountain regions is low and consequently it is found that the values of $\overline{v'_l \pi'}$ are very strongly dependent on the structure and position of the centres of the (mountain) anti-cyclonic flows relative to the highest points of the barriers. If the anti-cyclones were centred over the western slopes then $\overline{v'_l \pi'}$ was generally found to be positive with $\bar{K} \to K'$ and $\bar{P} \to P'$ indicated by the conversion terms involving π, the reverse being true if the centres lie over the eastern slopes. In the model results these transformations were found to oscillate in sign as the position of the anti-cyclone shifted relative to the central point of the barrier.

3. Initial results using single and double barrier systems

To illustrate some characteristic empirical latitudinal distributions of transient and stationary components of poleward fluxes of sensible heat and of westerly momentum, values given by Oort and Rasmusson (1971) are shown in Fig. 1; the significant contributions made by the stationary components in northern hemisphere winter conditions are clearly seen. One of the aims of our numerical experiments is to explain the underlying cause of the presence of the stationary components.

As in the work of Smith and Davies (1977) each model experiment was initialized from a condition of zonal flow with a mid-channel westerly jet, and a vertical shear in the velocity field, with a suitable meridional temperature gradient. For experiments with no mountains baroclinic activity was started by imposing random perturbations on this zonal flow. With mountain barriers present, these immediately activated cyclogenesis in their downstream regions.

Some interesting results were noted in the first set of experiments, with $\eta = 0$. These involved $i = 78$ grid points from west to east and $j = 26$ from south to north, the grid spacing being 400 km zonally and meridionally, with a channel of corresponding dimensions 31,200 km and 10,400 km. The parameter values were those used by Smith and Davies. In Figs. 2(a), 2(b), 2(c) and 2(d) we show the time variations of zonal and eddy kinetic energy for (a) a no-mountain model, (b) an east–west barrier of height 3000 km covering $36 \leqslant i \leqslant 48$, $9 < j < 17$ and centred on $i = 42$, $j = 13$, (c) a north–south barrier of height 1500 m covering $4 \leqslant i \leqslant 10$, $8 \leqslant j \leqslant 18$ and centred on $i = 7$, $j = 13$, and (d) both barriers present. The presence of mountain barriers (b) and

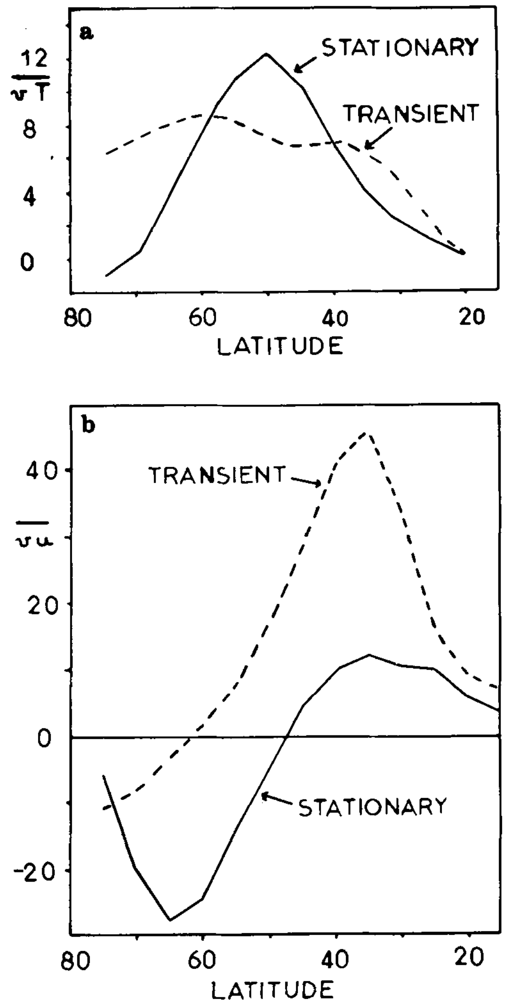

Fig. 1. (a) Vertically averaged northward flux of sensible heat ($\overline{vT}$ in m s^{-1} °C units) by large-scale eddies during January (as given by Oort and Rasmusson, 1971) as a function of latitude: —— stationary component, $[\overline{v'}][\overline{T'}]$; ------ transient component, $[\overline{v^{*\prime} T^{*\prime}}]$. (b) Northward flux of westerly momentum ($\overline{vu}$ in m^2 s^{-2} units) by large-scale eddies at 300 mb during January (Oort and Rasmusson, 1971), as a function of latitude: —— stationary component, $[\overline{v'}][\overline{u'}]$; ------ transient component, $[\overline{v^{*\prime} u^{*\prime}}]$.

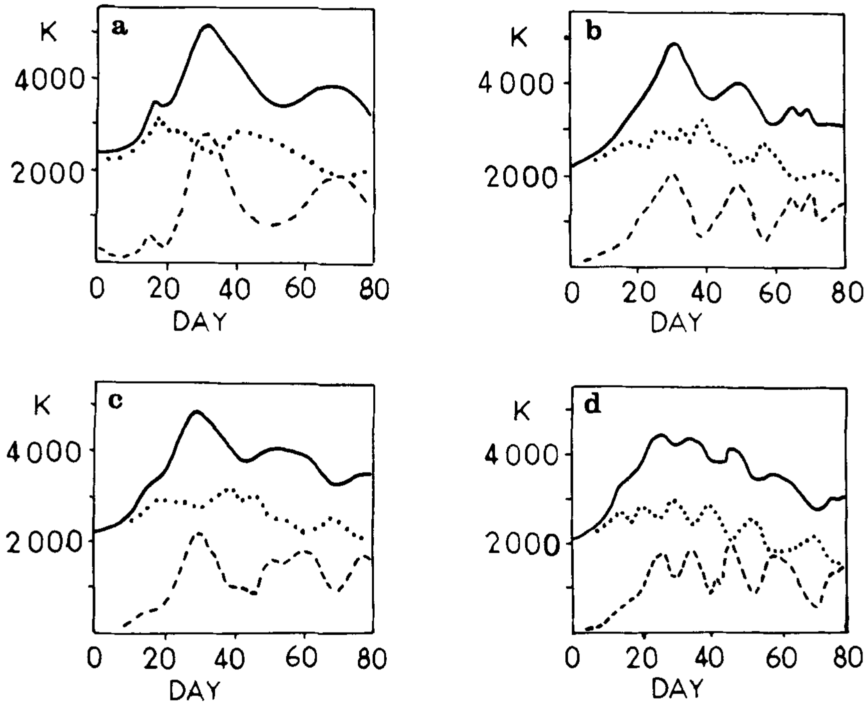

Fig. 2. Model kinetic energy (in units of KJ m^{-2}) for (a) no mountain barriers, (b) one E–W mountain, (c) one N–S mountain, (d) two mountains, of type (b) and (c) together. (Positions described in the text). —— K, ······ $\bar{K}$, ------ K'.

(c) is seen to lead to a reduction of the long-term "period" of baroclinic activity, expressed in K', to about 20 days. With two barriers present, (d), this period of variation of K' was further reduced to about 15 days.

It was also interesting to note (Fig. 3) that at the start of the integration, using model (c), there was a rapid adjustment of the zonal flow, with the formation of an anti-cyclone over the north-western mountain slopes and a trough over the south-eastern slopes. These intensified, the anti-cyclone moving slightly eastward so that it was centred over the barrier whilst the area of low pressure drifted downstream, creating a wave in the flow. This wave intensified over the next few days as the depression moved down channel, developing baroclinically under the effect of the imposed meridional temperature gradient, eventually reaching the next (cyclic) barrier downstream by day 10, a complex interaction with the stationary (barrier) anti-cyclone ensuing: this intermittency of cast off cyclonic systems and downstream development may lie behind a result referred to in Section 4 (involving the phasing of eddy kinetic energy in a partitioned domain) and in an analysis in Section 5 of atmospheric data.

In these initial experiments it was noted that the time variation in the K' function was much more regular than that in the actual atmosphere or in other models of similar type. Extension of the east–west extent of the model produced a stronger cycle of activity with longer periods of variation. In order to further improve the model in this respect the inclusion of the term $\eta(\mathbf{v}_s \cdot \nabla)\pi$ was also tested, using values of η corresponding to previously used parameters. Although an increase of 20% in computing time resulted, several improvements were noted: there was a greater degree of variation in K' and ∇T (the meridional temperature gradient); a greater meridional variation in the positioning of cyclonic systems and a stronger stationary wave throughout the domain.

Using a non-zero η value, with a spatial model domain of $i = 88$, $j = 26$, zonal and meridional grid spaces of 350 km and 325 km, and two mountain barriers of the same heights and relative

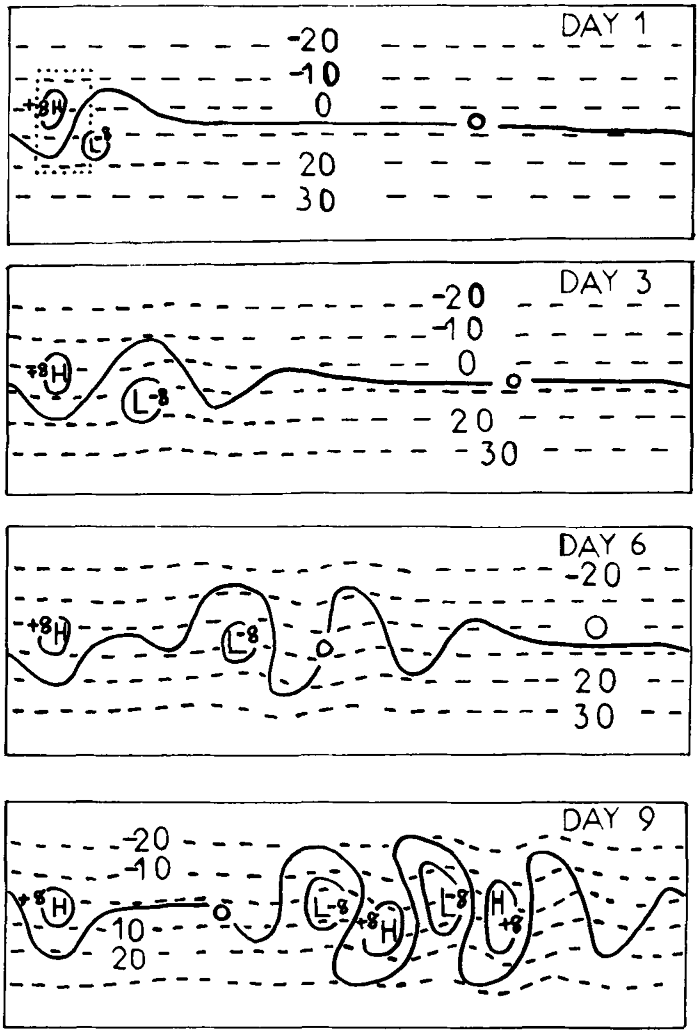

Fig. 3. Initial integration (days 1, 3, 6, 9) using model (c) of Fig. 2 (one N–S barrier, marked at day 1 by ······): 500 mb temperature in °C ------; deviations in mb of surface pressure from 1000 mb ——.

positions used in the first experiments, a comparison of mountain and no-mountain barrier results was again made, as shown in Figs. 4(a), 4(b), 4(c), 4(d). These relate to stationary and transient components of northward fluxes of sensible heat and of westerly momentum, averaged over a 30-day period. The stationary components are negligible for both quantities in the no-mountain model; the results for the mountain case are, however, similar in general shape to the observed distributions (Fig. 1), illustrating the importance of planetary scale mountain barriers in creating general circulation characteristics. Other marked differences were noted: for example, the meridional circulations differed considerably. In the mountain model both Hadley and Ferrel cells were much more intense than in the no-mountain model, peak velocities being 70 cm s^{-1} compared to 20 cm s^{-1}, and 60 cm s^{-1} compared to 40 cm s^{-1} respectively. The presence of barriers was also seen to create regions of divergent motion over the west and north-west mountain slopes and regions of convergent motion over the east and south-east slopes, a balance being formed by

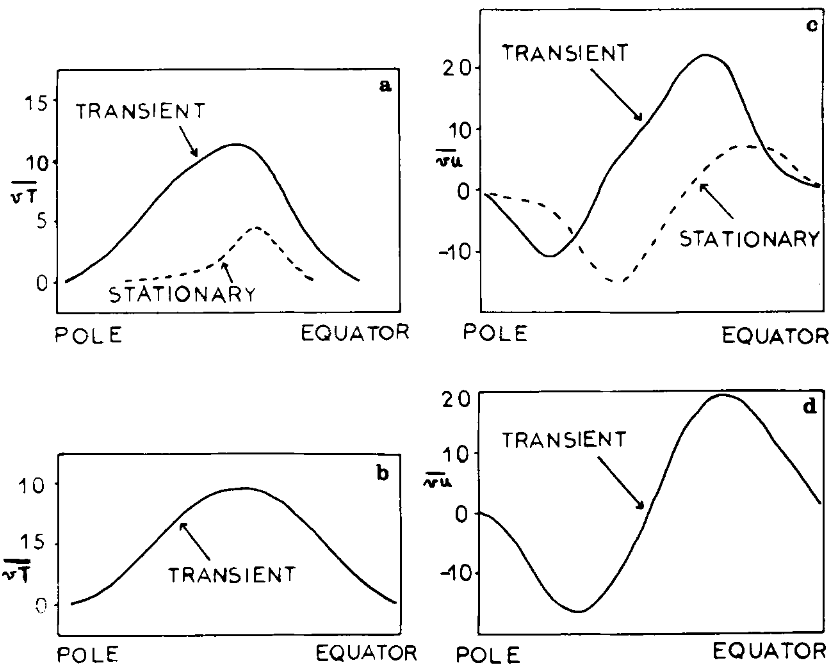

Fig. 4. (*a*) *and* (*b*): Northward flux of sensible heat ($\overline{vT}$ in m s^{-1} °C units) due to large-scale eddies in the model: 4(a) relates to a two-mountain model (described in the text); 4(b) relates to a no-mountain model. Stationary components are negligible in (b). ------ Stationary component, $\overline{[v'][T']}$; —— transient component, $\overline{[v^{*\prime}\, T^{*\prime}]}$. (*c*) *and* (*d*): Northward flux of westerly momentum ($\overline{vu}$ in m^2 s^{-2} units) by large-scale eddies in the model: (c) relates to a two-mountain model (described in the text); (d) relates to a no-mountain model. Stationary components are negligible in (d). ------ Stationary component, $\overline{[v'][u']}$; —— transient component, $\overline{[v^{*\prime}\, u^{*\prime}]}$.

advection of cold air southward over the eastern slopes and of warm air northward over the western slopes. This sensible heat flux was achieved by the anti-cyclonic circulation formed in the vicinity of the mountain. The introduction of a barrier (either north–south or west–east) also caused a northward shift of the jet stream and usually produced a narrower and more intense jet. There was also a northward shift in the position of the maximum meridional temperature gradient.

An analysis of the energy transformation emphasizes further the influence of the barriers. Fig. 5 shows the computed time variations over a period of 30 days (from day 81 to 110) of the internal energy conversion $\{\bar{K}\cdot K'\}$, as defined in (17), and the π component of this, $\{\bar{K}\cdot K'\}_\pi$, as defined in (19): Fig. 5(a) refers to the mountain model and Fig. 5(b) refers to the no-mountain model. In the latter case the π component is of the same sign as the internal component and a significant fraction of this. In the mountain case the variation is much more irregular, as we would expect, and the π component is not always of the same sign.

This result illustrates the fundamental influence of the barriers in model dynamics and suggests a similar result holds in certain regions of the real atmosphere. Fig. 6, (a) and (b), show that the contribution of the π component to conversions of $\{\bar{P}\cdot P'\}$ type are small: this is presumably due to the fact that the main overall factor here is the meridional heating gradient, imposed and kept fixed in the model. The significant contribution which the π component of kinetic energy conversion makes to the total energy exchanges is a reflection of the use of σ coordinates, forcing the model atmosphere into large-scale lateral and vertical motions around and over the barrier systems. This is not possible to achieve significantly in p coordinate models, and illustrates the advantage of σ coordinate systems.

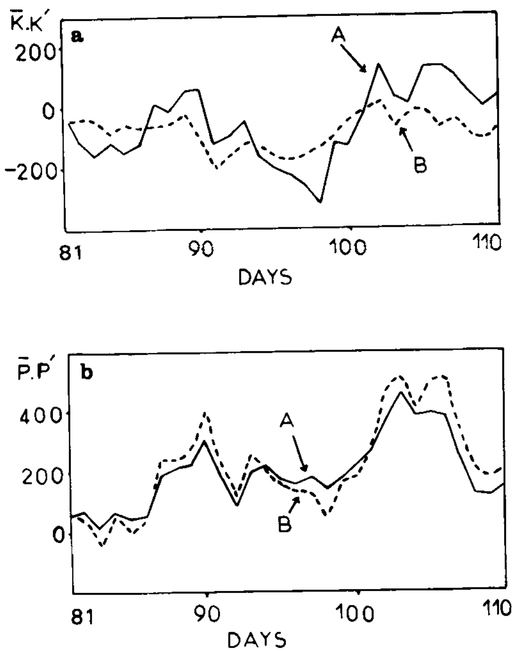

Fig. 5. (a) Model kinetic energy transformations (as defined in the text) for a two-mountain model (described in the text), in units of KJ m^{-2}: A, ——, $\{\bar{K}\cdot K'\} + \{\bar{K}\cdot K'\}_\pi$; B, ------, $\{\bar{K}\cdot K'\}$. (b) Model potential energy transformations (as defined in the text) for the two-mountain model, in units of KJ m^{-2}: A, ——, $\{\bar{P}\cdot P'\} + \{\bar{P}\cdot P'\}_\pi$; B, ------, $\{\bar{P}\cdot P'\}$.

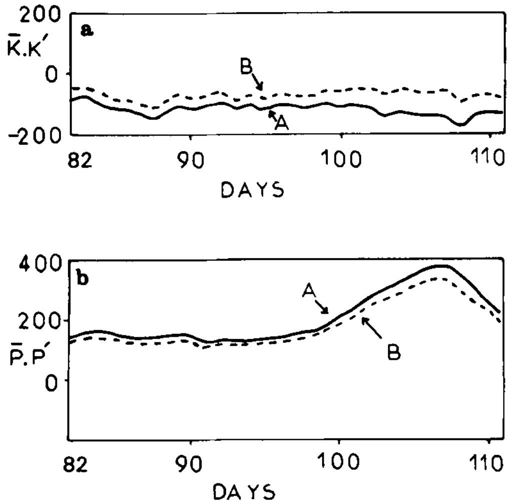

Fig. 6. (a) Model kinetic energy transformation for the no-mountain model, in units of KJ m^{-2}: A, ——, $\{\bar{K}\cdot K'\} + \{\bar{K}\cdot K'\}_\pi$; B, ------, $\{\bar{K}\cdot K'\}$. (b) Model potential energy transformations for the no-mountain model, in units of KJ m^{-2}: A, ——, $\{\bar{P}\cdot P'\} + \{\bar{P}\cdot P'\}_\pi$; B, ------, $\{\bar{P}\cdot P'\}$.

4. Further experiments

4.1. *Comparison of a no-mountain, land-sea differentially heated model with a mountain model*

A long-standing problem in meteorology is to determine the relative significance of contributions which (i) the deflection effects of the mountain barrier, and (ii) the land-sea zonally differentiated heating, make to the stationary components of poleward flux of sensible heat and westerly momentum. In the case of (ii), with no mountains, the heating function used was as simple as possible, varying linearly between the model equator and pole. The zonal extent of the channel was divided in two, one half representing the "sea" by a heating function $\dot{Q}_2$ varying linearly from zero at the "pole" to $+9.2 \times 10^{-3}$ J kg^{-1} s^{-1} at the equator, the other half representing the "land" by a heating function $\dot{Q}_2$ varying linearly from -9.2×10^{-3} J kg^{-1} s^{-1} at the pole to 0 at the equator, these functions having the same meridional gradient as the single function $\dot{Q}_2$ used in other experiments. The difference between the "land" and "sea" heating was large in order to produce a large east–west heating contrast, with the aim of producing an intense stationary field.

However, in a long time integration the expected stationary component of poleward flux of sensible heat did not appear: it was negligible compared with the strong stationary values produced in the mountain models discussed in Section 3. In Fig. 7 a typical distribution of 30-day averaged (day 131 to 160), sea level isobars and 500 mb isotherms is shown. A strong stationary pattern of the former is noted, with a large preferred area of low pressure being situated over the northern part of the "sea" area and two small regions of high pressure over the north–east and south–east of the "land" area. Although day to day cyclonic flows were generated in a conventional model fashion, no significant temperature stationary wave appeared in a 30-day average; there was only a slight southward shift of the isotherms over the land. This resulted in the northward fluxes of heat and of

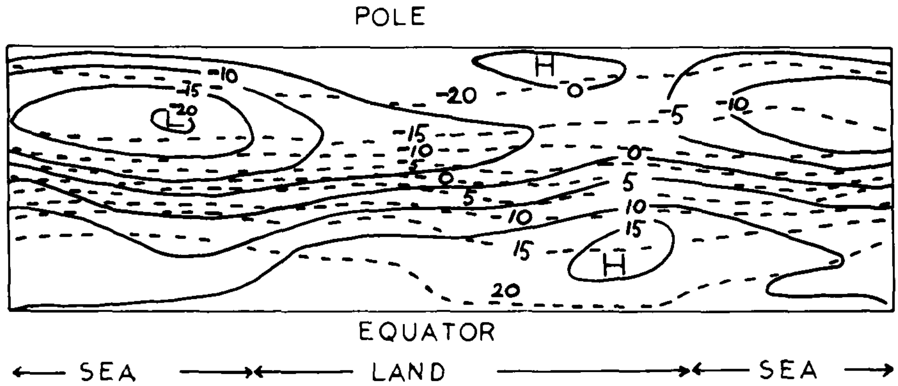

Fig. 7. Distribution of 30-day averaged (day 131 to 160) sea level isobars (mb deviation from 1000) and 500 mb isotherms (°C) for the no-mountain model but with longitudinal heating contrasts (described in the text).

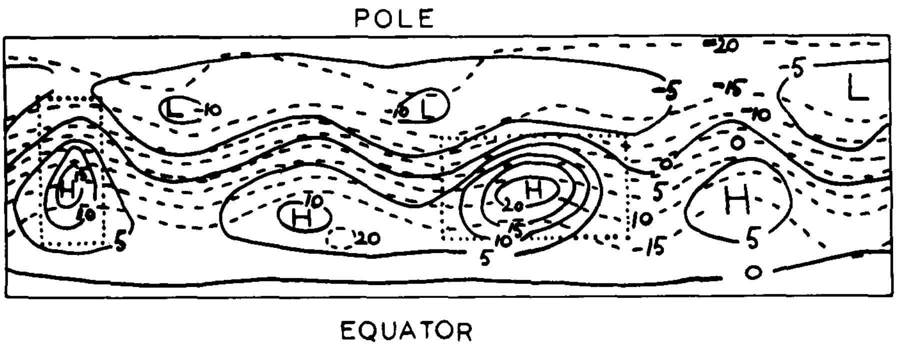

Fig. 8. Distribution of 30-day averaged (day 161 to 190) sea level isobars (mb deviation from 1000) and 500 mb isotherms (°C) for the two-mountain model (defined in the text): position of barriers indicated ······.

westerly momentum exhibiting only very small stationary components. This strongly suggests that it is the orographic factors which are of greatest importance for the production of stationary components of these fluxes, and that the direct thermal influences on the stationary characteristics are relatively small.

In order to emphasize the totally different results produced by the presence of mountain barriers, typical distributions of 30 days (day 161–190) averaged, sea level isobars and 500 mb isotherms are again shown (Fig. 8). The positions of the two barriers are indicated; in order not to exaggerate the barrier effects the "Rockies" barrier was taken to be 1000 m high only (centred on $i = 10, j = 13$, covering 6×14 grid points) and the "Himalayas" barrier was taken to be 1500 m high (centred on $i = 55, j = 11$, covering 10×18 grid points); the numerical values of the basic physical parameters of the model were otherwise the same as in the no-mountain model of Fig. 7. The stationary nature of both mean isotherms and pressure are clearly seen: a preferred cyclogenesis region appears to the north–east of the "Rockies" (as in Smith and Davies, 1977) but the preferred cyclogenesis region associated with the Himalayas appears to the north–west of the barrier position.

Some interesting (and possibly significant) results were also noted in analyses of individual days. At day 172 (Fig. 9a), for example, the

Fig. 9. Distribution of sea level isobars (mb deviation from 1000) and 500 mb isotherms (°C) for the two-mountain model (defined in the text) for days 172, 176, 177 and 179: positions of barriers indicated ······; equator and pole positioned as in Fig. 8.

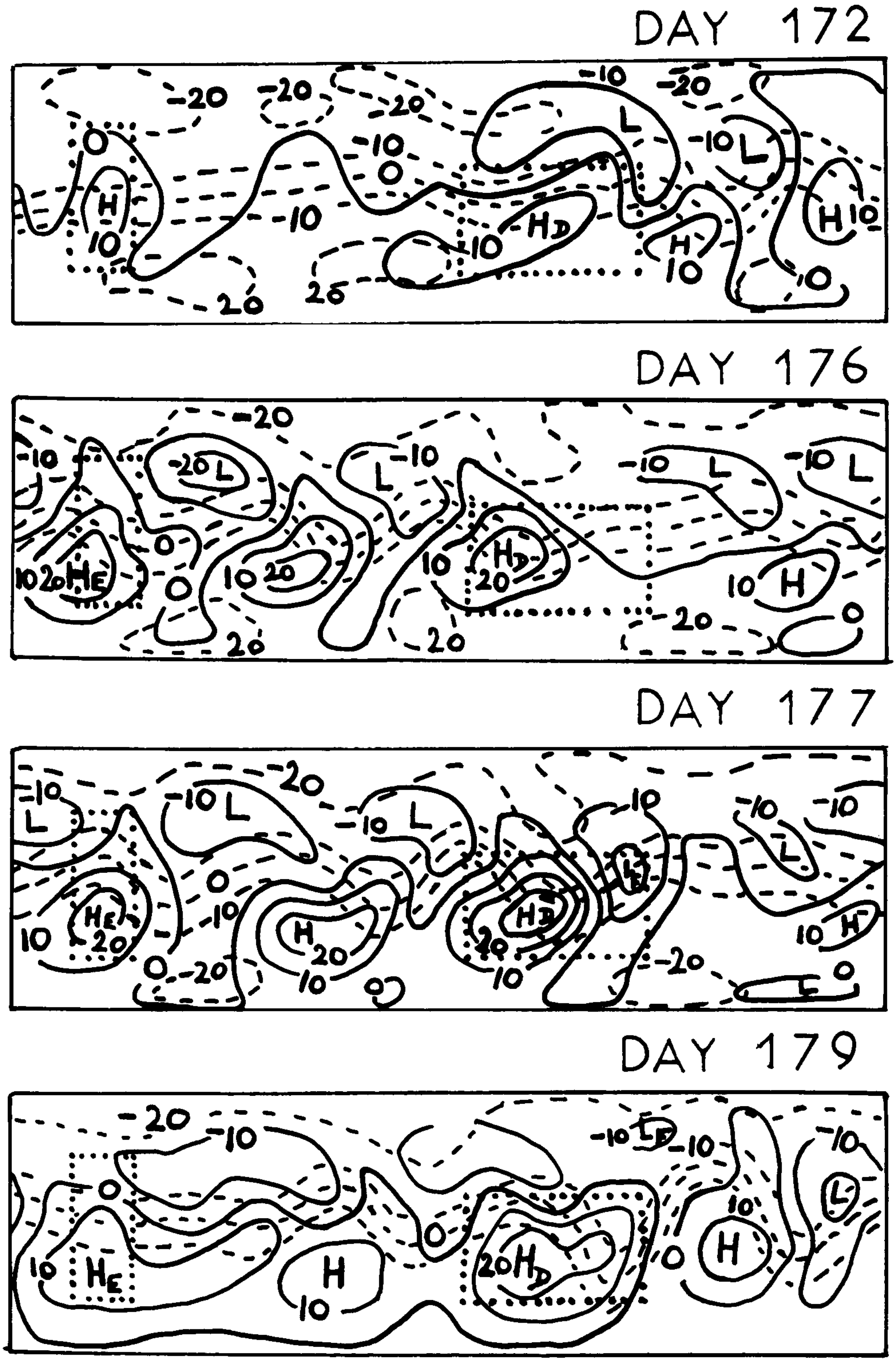

a

b

c

d

pressure systems were weak throughout the domain, with anticyclones situated over the barriers, dynamical activity being largely confined to the eastern half where there was a relatively strong temperature wave; elsewhere the isotherms were predominantly aligned east to west. By day 176 (Fig. 9b) a reversal of the distribution of activity had taken place, so that the isotherms now showed most meridional movement in the western half of the channel. High D had shifted westwards so that its positioning relative to the temperature wave promoted a strong poleward flux of sensible heat. Both high-pressure systems D and E were centred over the western slopes of the barriers suggesting that their contributions to the transformation $\{\bar{K} \cdot K'\}_\pi$ is positive: in fact a change from negative to positive occurred between days 176 and 177. Day 177 (Fig. 9c) is interesting in showing a rapid intensification of high D accompanied by the formation of low F over the north-eastern slopes of the zonally oriented range, which was also a region of high temperature gradient on this occasion—a good example of lee cyclogenesis in the model. It is also interesting to note that the position of the temperature wave relative to anticyclone D and depression F is such as to result in a strong poleward flux of sensible heat. By day 179 (Fig. 9d) the dynamical activity had decreased as low F drifted north eastward and decayed: the pressure systems were spatially larger but less intense.

The most striking characteristic of the flow patterns was that the temperature wave retained its form while progressing eastwards. The model dynamics was in its most active phase in the vicinity of this temperature wave, the pressure distributions producing strong northward transfer of sensible heat. Although there was always a clear anti-cyclonic tendency in the region of the barrier, the exact positioning of these anti-cyclones strongly influenced the temperature wave.

4.2. *Comparison of the phasing of energy time variations in the western and eastern halves of a mountain model*

The alternation of peak dynamical activity between the western and eastern halves of the model suggested that a computation over a long period of time of the partitioning of eddy kinetic energy into western and eastern halves would be of interest. A search for a basic approximate periodicity due to this factor might be related to long-term studies of quasi-periodic variations in planetary scale atmospheric behaviour, by, for example, Namias (1954), Quinet (1974), McGuirk and Reiter (1976). Also, it is interesting to note that Winston and Krueger (1961) examined the daily variation of available potential energy in four equal zones of the northern hemisphere for the period 21 December 1958 to 13 January 1959. There was clear evidence of a strong cycle of activity over America and the western Atlantic, with no similar feature in any of the other zones. In this case the overall atmospheric behaviour was strongly dependent on activity in this one area.

Consequently, as an initial attempt to study some of the regional aspects of energy variation, evaluations were made of the kinetic energies in the western and eastern halves of a model channel, the barrier being a north–south type, 1500 m high, centred on $i = 50$, $j = 13$ and covering 6×9 points, in the eastern half.

In Fig. 10 some typical results of an analysis are shown, K'_1 and K'_2 representing the eddy kinetic energy variations with time in the western and eastern halves of the channel respectively. The dominant characteristic is that maxima in K'_1 are approximately in step with minima in K'_2 and vice-versa, so that generally increasing (or decreasing) K'_1 is associated with decreasing (or increasing) K'_2. This apparent east–west oscillation of eddy kinetic energy recurred between periods of minima in total eddy kinetic energy $(K'_1 + K'_2)$ over the whole range of time integration. A further analysis, splitting the channel into four equal zones, showed also that an initial peak of K' forming initially in the region containing the barrier was followed in time by a peak in the next zone downstream, subsequent maxima then occurring in the other two areas. It appeared that a "packet" of baroclinic energy formed in the zone containing the barrier and then propagated eastwards, approximately retaining its localized dynamical characteristics. A similar "wave packet" effect had been observed (Fig. 3) to be produced by the initialization of the system when a mountain barrier was included, and was also apparent at certain times in continuous sequences of flow

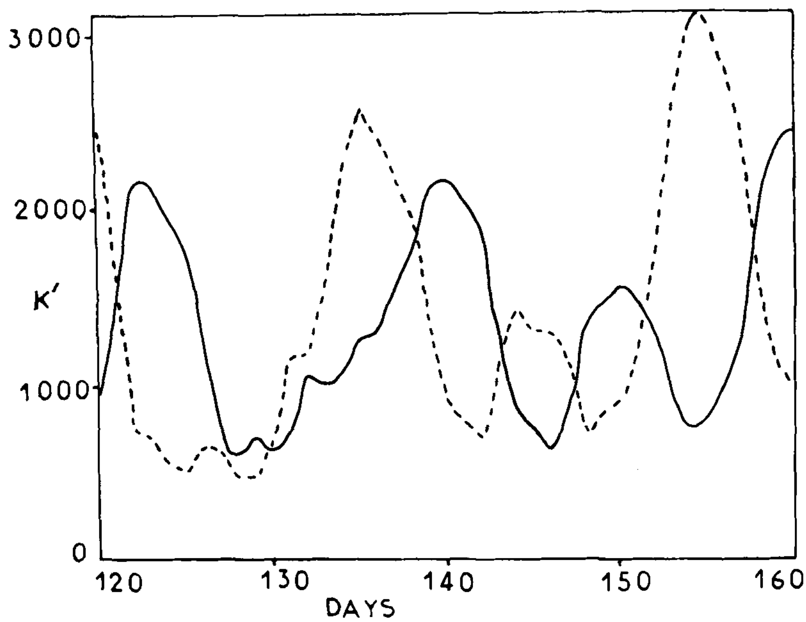

Fig. 10. Variation with time (from day 120 to day 160) of partitioned eddy kinetic energy (units of KJ m^{-2}) in the model defined in the text ——, K'_1, for region 1; -----, K'_2, for region 2.

charts of the type shown in Fig. 9, associated with the tendency of the temperature wave to retain its form during its progress across the channel.

The following physically plausible explanation is consistent with these results. Beginning the argument from the context of a model state of low baroclinic activity, and a correspondingly small domain K' value, an increasing meridional temperature gradient sets up critical conditions for baroclinic instability and cyclogenesis forms, producing a strong poleward flux of sensible heat which in due course reduces the meridional temperature gradient throughout the channel. This then lessens the likelihood of strong baroclinic instabilities forming elsewhere in the model domain. Therefore, most of the dynamical activity occurs initially in one part of the domain and drifts downstream with the west–east flow, developing as it moves and so gives rise to the energy oscillation seen in Fig. 10. Eventually the total K' reaches a minimum, and the cycle is repeated. In experiments without orography there were no preferred areas for the initial instability and a partitioning of eddy kinetic energy into a K'_1 and K'_2 form, although generally out of phase, were of approximately the same amplitude. But with a barrier present in region 2, the initial instability could be identified with lee cyclogenesis, resulting in the initial peak in K' occurring always in region 2.

It has been noted by Gates (1961) that the two parameter quasi-geostrophic model has a tendency to over-estimate the growth of mature disturbances whilst suppressing the development of new activity. However, these model results demonstrate that strong dynamical activity in one part of the channel frequently inhibits baroclinic growth in other parts. In the real atmosphere there are, of course, no lateral walls and we would not anticipate an exactly similar phenomenon. However, similar general effects could be produced. For example, a strong poleward flux of sensible heat in the western part of the northern hemisphere would tend to warm the polar air and could lead to a lessening of the meridional temperature gradient in the eastern half of the northern hemisphere. The effect of this could be similar to that enforced in the β-plane model by the model wall boundary conditions.

To test whether these model results had relevance to the real situation, an analysis of the energetics of the real atmosphere was carried out.

5. An analysis of some atmospheric data

The data used was supplied by the U.K. Meteorological Office and covered the years 1961–63; this period was selected as it contained the exceptional U.K. winter of 1962–63, although unfortunately no data was available for a part of the Pacific region and so the analysis was restricted to the remainder of the northern hemisphere troposphere. The data consisted of the 500 mb height and the 1000–500 mb thickness values at points on a grid with intervals of 5° in latitude and 10° in longitude. These geopotential heights were used to evaluate geostrophic velocities at 500 mb and hence to estimate the kinetic energy, with partitioning into zonal and eddy components. The 750 mb temperature distribution was approximated from the thickness and a measure of meridional temperature gradient obtained.

In the model results, the kinetic energy, summed over levels 1 and 3, is given by $K = \frac{1}{2}m(u_1^2 + u_3^2 + v_1^2 + v_3^2) = K_m + K_s$, where $K_m = (m/2)(u_2^2 + v_2^2)$. $K_s = (m/2)(u_s^2 + v_s^2)$, $u_s = \frac{1}{2}(u_1 - u_3)$, $v_s = \frac{1}{2}(v_1 - v_3)$, $u_2 = \frac{1}{2}(u_1 + u_3)$, $v_2 = \frac{1}{2}(v_1 + v_3)$ and $m = \pi/g$. K_m relates to the kinetic energy of the mean flow, and K_s is associated with the vertical shear of the wind field. In our analysis of atmospheric data we were able to calculate K_m only and so our calculated kinetic energies (eddy and zonal components) for the atmosphere would tend to have lower values than those obtained from equivalent model calculations.

Two partitioned zones were defined; the first (region 1) included North America, the Atlantic and Western Europe (110° W–10° E); the second (region 2) extended over the remainder of the Eurasian Continent (10° E–140° E). Their size and position were determined by the areas of available data for 1961–63. The areas were restricted meridionally to the latitude belt between 40° N and 65° N; despite these restrictions it was felt that these limited areas would be sufficient to indicate the general relative trends of time changes in the partitioned energy of the two areas.

The time variation of $K' \cdot \bar{K}$ and ∇T (zonal average of the difference between the 750 mb temperature at 40° N and 65° N) was evaluated for the winters of 1961–62 and 1962–63. The value of K' in region 2 (east) was usually found to be less than that in region 1 (west), a consequence of the area of high pressure dominating the Eurasian Continent for most of the winter months: this was also true for $\bar{K}$ and ∇T. These variations showed much more irregularity than those produced by the model, which reflects only the large-scale flow characteristics. The analysis also shows K' and $\bar{K}$ to be almost exactly out of phase, with minima (maxima) in ∇T generally occurring only 1–2 days after maxima (minima) in K', this being a characteristic also of a model with a mountain present, although results for the model without mountains produced a lag of 5–6 days.

An examination of $K'(t)$ for regions 1 and 2 show that there were distinct periods in which K_1' was clearly out of phase with K_2'; in other periods they were, however, closely in phase (see Fig. 11). To classify these two modes of activity, the sign of $\Delta K_l'$ ($l = 1$ or 2), the daily change of eddy kinetic energy in each zone l, was noted and also the sign of $S = \Delta K_1' \times \Delta K_2'$. If S is positive then $K'(t)$ is following the same trend in each zone (i.e., either rising or falling in each), whilst if S is negative then $K'(t)$ is increasing in one zone and decreasing in the other. The winter of 1961–62 produced excellent examples of these different types of behaviour and in Table 1 the values taken by S throughout the period are shown.

These results show that there were definite times when K_1' and K_2' were either predominantly in phase or out of phase: periods A, C, E were of the first type and were unlike the model results, but periods B, D and F were of the second type, with properties similar to those displayed by the model. In A, C, E the atmosphere's build-up or break-down of kinetic energy was in phase across the two regions, the variation in the associated meridional temperature gradient showed similar in-phase behaviour. However, the model type of behaviour, with out of phase changes in eddy kinetic energy, is also seen from Table 1 to occur substantially in the atmosphere over the period tested.

An analysis of the zonally averaged 750 mb temperature field shows it is associated with these energy oscillations in the atmosphere. In Fig. 12

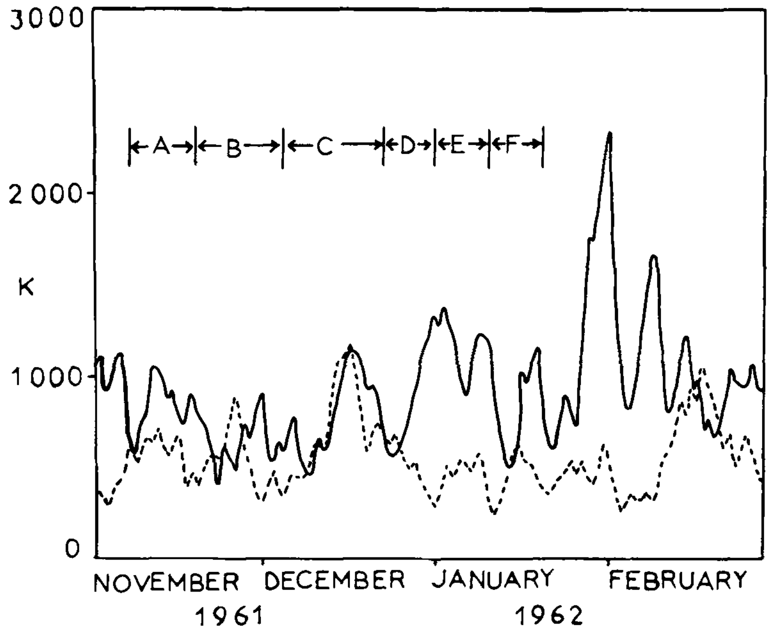

Fig. 11. The time variation of partitioned eddy kinetic energy (in units of KJ m^{-2}) during the winter of 1961–62: ——, K_1'; ------, K_2'. The periods A–F are defined in Table 1 of the text: K_1' for region 1 and K_2' for region 2.

Table 1. *Division of winter of 1961–62 into periods during which K_1' and K_2' are either predominantly in or out of phase*

Period	First day	Last day	Number of days when $S > 0$	Number of days when $S < 0$	Dominant phasing
A	6.11.61	17.11.61	9	3	IN
B	18.11.61	3.12.61	3	13	OUT
C	4.12.61	22.12.61	15	4	IN
D	23.12.61	31.12.61	1	8	OUT
E	1.1.62	9.1.62	7	2	IN
F	10.1.62	18.1.62	1	8	OUT

these temperature distributions for regions 1 and 2 are shown: the periods defined in Table 1 are marked. During the "in phase" period C (4–22 December, 1961) it is interesting to note that the structure of the isotherm distribution was similar in the two zones. However, for the "out of phase" period F (10–18 January, 1962), for example, the isotherm distributions for the separate regions were strikingly different. In zone 1 a cold air mass moved southwards from the north of the region intensifying the temperature gradient and encouraging the development of baroclinic activity. In zone 2 the opposite situation was noted with a lowering of meridional temperature gradient.

These variations in phasing of K_1' and K_2' seemed to be reflected also in the orientation of the major axis of the polar vortex, particularly at times of transition from an in phase to an out of phase mode. The charts studied were those produced by the U.S. Weather Bureau and gave the temperature and geopotential heights of the 500 mb surface in high latitudes. It is interesting to compare the general orientation of the polar vortex on, for example, 5 December (Fig. 13a) with that on 23 December (Fig. 13b), the former date coming at the beginning of an "in phase" period C, and the latter at the beginning of an "out of phase" period D. On 5 December

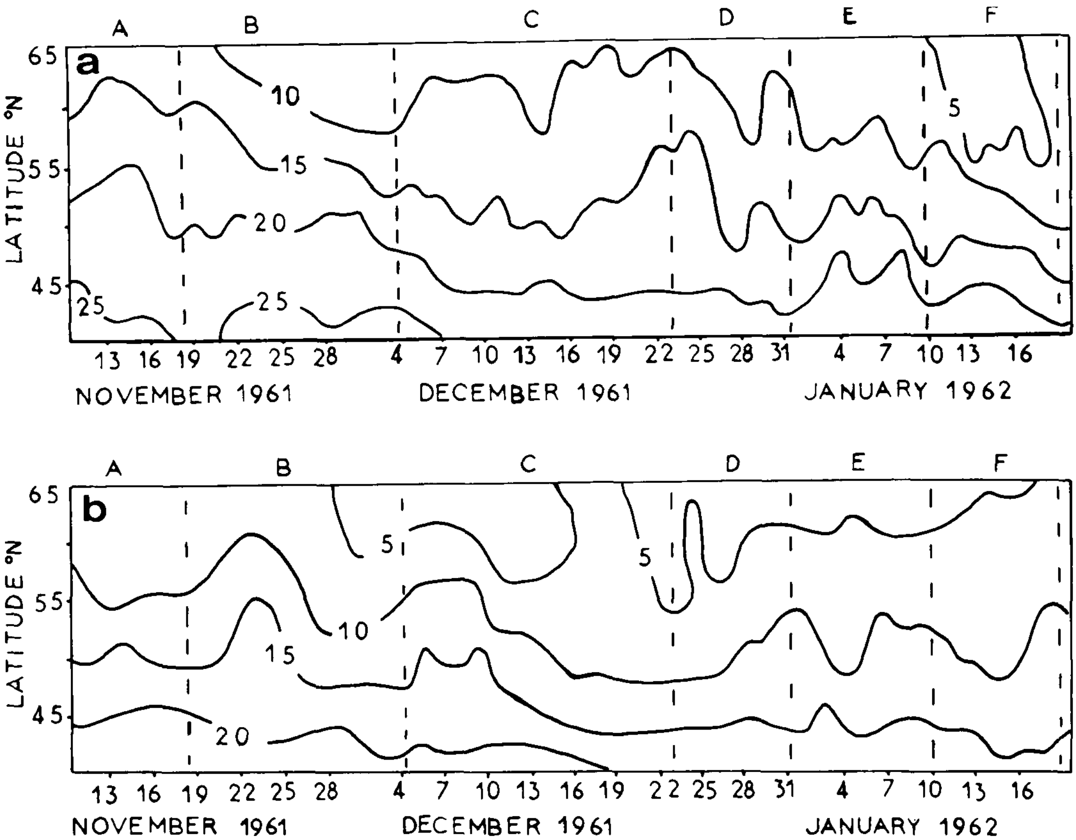

Fig. 12. The time variation of the latitudinal (°N) distribution of 750 mb isotherms (°C), averaged over (a) region 1, and (b) region 2, for the winter of 1961–62: the periods A–F are as defined in Fig. 11.

the major axes of the cyclonic systems, defined by the 168 height contours (in hundreds of feet), and the larger system, defined by the 176 contour, are orientated parallel to a line running approximately from 40°W to 140°E. By 23 December, however, they are parallel to the line 45° E to 135° W. Charts for intermediate days show that soon after 5 December the orientation settles down at 80° W–100° E and the swing to a 135° W–45° E line took place on 20 December. It was also interesting to note that in all cases studied the highest meridional temperature gradients occurred along these axes.

This analysis of data (although limited) for the period 1961–63, following up the results of the model numerical experiments, indicates that substantial oscillation of northern hemisphere eddy kinetic energy into east and west partitions takes place in winter time and that the orientation of the polar vortex is related to this. Extension of this analysis to other more recent years, for which more exhaustive detail is available, is needed and a relationship sought for between this oscillation and cyclogenesis processes in the lee of planetary scale mountain barriers.

6. Conclusions

Several new model results have been obtained by carrying out numerical experiments using a σ-coordinate, β-plane, quasi-geostrophic system, including a representation of planetary scale mountain barriers.

(i) It was found that when the total model eddy kinetic energy, $K'(t)$, was partitioned into components associated with the western and eastern halves of the region (the eastern half

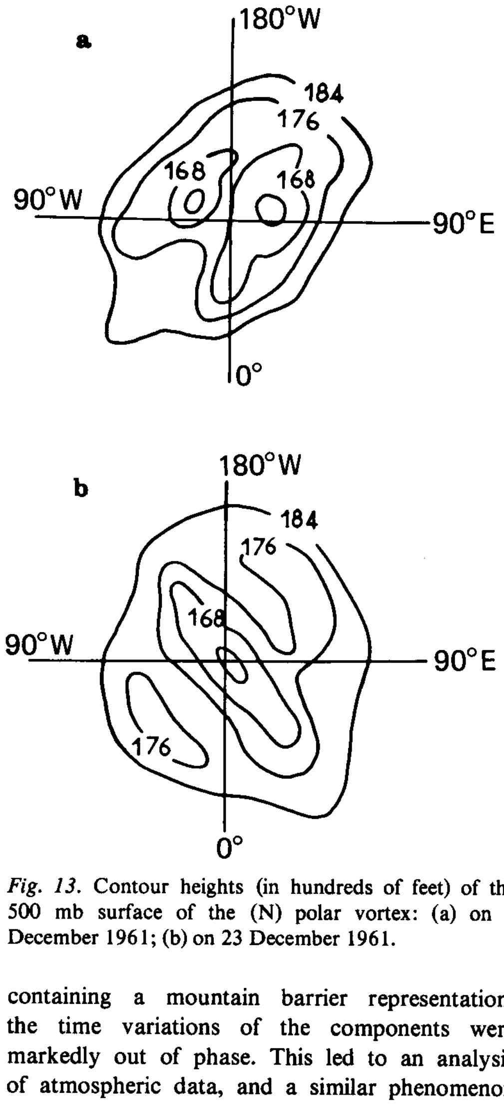

Fig. 13. Contour heights (in hundreds of feet) of the 500 mb surface of the (N) polar vortex: (a) on 5 December 1961; (b) on 23 December 1961.

containing a mountain barrier representation) the time variations of the components were markedly out of phase. This led to an analysis of atmospheric data, and a similar phenomenon was identified for the winter seasons of the years 1961–63, with distinctive periods of both phasing and anti-phasing in the eddy kinetic energy, as evaluated for the western and eastern zones. This also appeared to be related to the positioning of the polar vortex in the northern hemisphere. It is suggested that these types of behaviour are related to definite modes of atmospheric activity in which the large-scale mountain barriers tend to act so as to anchor dynamically stable distributions of pressure.

(ii) The numerical experiments showed that, in the model, orographic forcing is certainly a much more important factor than east–west thermal forcing in producing the stationary components of poleward transports of sensible heat and westerly momentum. The orographic forcing led to the formation of stationary components which were generally similar to those observed in the actual winter hemisphere. However, experiments with no mountain barrier effects but with strong east–west thermal contrast (representing the land–sea climatological, zonal, winter temperature difference) produced only very small stationary components of the poleward fluxes.

(iii) The energy cycle of the model atmosphere was considerably altered by the inclusion of mountain barriers. The positioning of pressure systems relative to these barriers was generally found to be such that at times of high baroclinic activity (K' high), those parts of the atmosphere in the region of the mountains contributed a large proportion of the total poleward transfer of sensible heat. However, during the periods when the atmosphere was relatively inactive (i.e., K' low), the flux of sensible heat was frequently found to be in an equatorward direction. Thus the effect of the orographic forcing was to accentuate the rates of change in the mid-channel meridional temperature gradient, thereby increasing both the amplitude and the frequency of the associated baroclinic cycle, expressed in terms of K'.

The division of the energetics analysis of the model into two parts also yields an interesting new result; one part is associated with mid-tropospheric flow and the other (represented by energy transformation terms of the type $\{\bar{K}\cdot K'\}_\pi$) is associated with the direct effect of the mountain barrier surface in diverting air flow. The contribution of the latter to the conversion of kinetic energy between eddy and zonal forms is seen to depend on the relative positions of barriers and their associated anti-cyclonic flow systems.

All these results suggest that a more intensive study of relevant atmospheric data for recent years, where more complete data are available, would be fruitful. Time variations in regional weather characteristics are likely to be closely related to these processes; it is clearly an important factor to be represented in climatic change modelling.

7. Acknowledgements

P. Langley gratefully acknowledges the financial aid of a NERC (U.K.) Research Studentship.

We are also grateful for the assistance given by staff of the Exeter University Computer Unit and for the supply of various atmospheric data by the U.K. Meteorological Office. A part of this paper was presented at the 1978 European Geophysical Society Meeting at Strasbourg.

REFERENCES

Egger, J. 1976. On the theory of the steady perturbations in the troposphere. *Tellus 28*, 381–389.

Fultz, D. et al. 1959. Studies of thermal convection in a rotating cylinder with some implications for large scale atmospheric motions. *Meteor. Monogr. 24, Amer. Meteor. Soc.*

Gates, W. L. 1961. The stability properties and energy transformations of the two-layer model of variable static stability. *Tellus 13*, 460–470.

Lorenz, E. N. 1955. Available potential energy and the maintenance of the general circulation. *Tellus 7*, 157–167.

Manabe, S. and Terpstra, T. B. 1974. The effects of mountains on the general circulation of the atmosphere as identified by numerical experiments. *J. Atmos. Sci. 31*, 3–42.

McGuirk, J. P. and Reiter, E. R. 1976. A vacillation in atmospheric energy parameters. *J. Atmos. Sci. 33*, 2080–2093.

Namias, J. 1954. Quasi-periodic cyclogenesis in relation to the general circulation. *Tellus 6*, 8–22.

Oort, A. H. and Rasmusson, E. M. 1971. Atmospheric circulation statistics. NOAA, Prof. Pap. No. 5.

Phillips, N. A. 1956. The general circulation of the atmosphere: a numerical experiment. *Q. Jl. R. met. Soc. 82*, 123–164.

Quinet, A. 1974. A numerical study of vacillation. *Adv. Geophys. 17*, 101–186.

Smith, R. F. T. and Davies, D. R. 1977. A note on some numerical experiments with model mountain barriers. *Tellus 29*, 97–106.

Winston, J. S. and Krueger, A. F. 1961. Some aspects of a cycle of available potential energy. *Mon. Weath. Rev. 89*, 307–318.

ЧИСЛЕННЫЕ ЭКСПЕРИМЕНТЫ С ПРОСТОЙ МОДЕЛЬЮ ВОЛН ЗА ГОРНЫМ БАРЬЕРОМ ПЛАНЕТАРНОГО МАСШТАБА

Для изучения влияния горных барьеров планетарного масштаба на василляции энергии и перенос тепла используется двухуровенная модель общей циркуляции на β-плоскости в б-координатах (размерами 10000 км по меридиану и 30000 в зональном направлении). Результаты численных экспериментов по моделям с плоской топографией (и контрастами нагрева море-суша) сравниваются с таковыми по моделям, описывающим Скалистые горы и Гималайи. Видно, что горные хребты имеют решающий эффект на временные вариации полной вихревой кинетической энергии K', меридиональные градиенты температуры ∇T и на создание стационарных компонент переноса к полюсу тепла и зональной компоненты импульса. Области предпочтительного формирования сильных меридиональных градиентов температуры и циклонических систем были к северо-востоку от Скалистых гор, но к северо-западу от Гималайев.

Когда величина K' была разделена на две, соответствующие западной и восточной половинам канала β-плоскости, то временные вариации K', связанные с каждой половиной, были часто несинфазны, увеличение $K'(t)$ в одной половине и уменьшение $K'(t)$ в другой были связаны с движущимися на восток пикамй бароклинной активности (возникающими вниз по течению от барьера). Аналогичный процесс был найден при анализе атмосферных данных за 1961–63 гг., причем ориентация полярного вихря была тесно связана с западно-восточными осцилляциями K'; результаты модели предполагают, что системы горных барьеров имеют большое влияние. Временные вариации в характеристиках региональной погоды представляются тесно связанными с этим процессом; ясно, что он является важным фактором, который должен найти отражение в моделировании изменений климата.